Modelling winter conditions of streets and pavements in a changing climate

Master's Thesis, 3.6.2019

Author:

Olli Saranko

Supervisors:

Carl Fortelius (FMI)
Topi Kähärä (JYFL)

UNIVERSITY OF JYVÄSKYLÄ
DEPARTMENT OF PHYSICS

Abstract

Saranko, Olli
Modelling winter conditions of streets and pavements in a changing climate
Master's Thesis
Department of Physics, University of Jyväskylä, 2019, 49 pages.

FMI's road weather model RoadSurf, weather model HARMONIE-AROME and surface modelling platform SURFEX with Town Energy Balance model TEB were used to model weather and especially road and pedestrian weather conditions in a changing climate in the Helsinki capital region. The grid resolution was 500 m for SURFEX/TEB and 2.5 km for HARMONIE-AROME. The simulated effects of climate change were based on the Representative Concentration Pathway RCP8.5 and several climate change models. The modelled time horizon was 2040–2069. The study is part of two EU-projects, URCLIM and iSCAPE.

The climatological changes are most significant in air temperature forcing. The model results show that the number of difficult road and pedestrian conditions decrease significantly. Both road and pedestrian conditions depend clearly on the urban morphology, but these dependencies are not very strong.

Keywords: RoadSurf, road weather, NWP, climate change, road conditions, pedestrian conditions, RCP8.5, 2055 climate, SURFEX, TEB, HARMONIE-AROME , URCLIM, iSCAPE

Tiivistelmä

Saranko, Olli
Tie- ja jalankulkuolosuhteiden mallintaminen muuttuvassa ilmastossa
Pro gradu -tutkielma
Fysiikan laitos, Jyväskylän yliopisto, 2019, 49 sivua

Ilmatieteen laitoksen tiesäämalli RoadSurfia, säämalli HARMONIE-AROME:a, ilman ja alustan vuorovaikutuksia kuvaavaa malliyhdistelmä SURFEX:ia ja kaupungin energiatasemalli TEB:iä käytettiin mallintamaan tulevaisuuden ilmaston tiesääolosuhteita Helsingissä ja pääkaupunkiseudulla. Käytetyn hilaruudukon tarkkuus oli SURFEX/TEB-mallilla 500 m ja 2,5 km HARMONIE-AROME-sääajoissa. Tiesää- ja jalankulkuolosuhteita tutkittiin erikseen RoadSurfin eri asetuksilla. Mallinnetut ilmaston muutokset perustuvat RCP8.5-kehityskaareen ja ilmastonmuutosmalleihin. Aikahorisontiksi valittiin 2040–2069. Tämä tutkimus on osa kahta EU-projektia, URCLIM:ia ja iSCAPE:a.

Mallien ennustamat sääolosuhteiden muutokset ovat merkittävimpiä ilman lämpötilassa. Mallinnetut tulokset osoittavat, että sekä vaikeat tieolosuhteet että liukkaat jalankulkuolosuhteet vähenevät merkittävästi. Sekä tiesää- että jalankulkuolosuhteissa näkyy selviä, mutta ei niin merkittäviä, riippuvuuksia kaupungin rakennustyypistä.
Avainsanat: RoadSurf, tiesää, keli, NWP, ilmastonmuutos, tiesääolosuhteet, jalankulkuolosuhteet, RCP8.5, 2055 ilmasto, SURFEX, TEB, HARMONIE-AROME, URCLIM, iSCAPE

Contents

1 Introduction

1.1 Winter road and pavement conditions in changing climate

Poor weather conditions are a common problem in Finland, especially during wintertime, for both pedestrians and car traffic. Snowfall can reduce visibility and increase the number of traffic accidents .[1] For pedestrians, most slipping accidents happen when there is either snow or water on top of ice.[2] Annual costs of these slipping accidents are approximately 2 400 million euros [3], and 427 million euros worth of compensations were paid for 95 000 traffic accidents in 2017, according to the report of the Finnish Crash Data Institute.[4] In 2006, the annual winter road maintenance costs per kilometer were 8 400–9 400 € for highways and 4 100–5 300 € for smaller roads [5], and for example, in 2016 the total winter road maintenance costs for the city of Tampere were five million euros [6].

As there is such a large amount of money involved, predicting winter conditions is in demand not only for current weather but also for the future climate. High-quality day-to-day forecasts are not available for longer than few weeks with current technology, but the development of the climate over decades can be estimated. These estimations can help to assess the road maintenance and health related costs in coming decades.

The effects of climate change on road conditions have previously been studied in Finland. De-icing and prevention of snow accumulation were estimated to be the most affected by climate change, when comparing to other aspects of road maintenance.[7] In 2006, Finnish Road Administration estimated[8] that the costs of ploughing and de-icing would decrease in Southern Finland, but in Central and Northern Finland, the costs of de-icing would increase while costs of ploughing would stay the same. In the same study, it was estimated that costs of renewing road pavements could increase by tens of millions of euros.[8]

This study aims to model the road and pedestrian conditions in a changing climate in the capital region of Helsinki, and to analyze how the changes are affected

by urban environment. The results of this study are for the use of city authorities as well as for two EU projects, iSCAPE and URCLIM. Numerical weather prediction model HARMONIE/AROME is used to model the meteorological conditions, and the influence of urban characteristics are factored in using Town Energy Budget (TEB) model in surface platform SURFEX. The effects of climate change are simulated according to RCP8.5 (Representative Concentration Pathway) trajectory. Finally, FMI's road weather model RoadSurf is used to model the road and pedestrian conditions of both recent and future climate.

1.2 iSCAPE

Project iSCAPE (*Improving the Smart Control of Air Pollution in Europe*) is funded by the European Community's H2020 Programme. The aim of iSCAPE is to develop technology related to improving air quality and reducing carbon emissions in European cities. Several research facilities from all over Europe have joined forces to create a consortium to tackle these issues.[9] One of the commissions for Finnish Meteorological Institute is to model the effects of climate change.

One part of iSCAPE has been the Living Labs that have been created in six cities around Europe. These cities are Bologna in Italy, Bottrop in Germany, Dublin in Ireland, Guildford in Great Britain, Hasselt in Belgium and Vantaa in Finland. These Living Labs have various ways to develop interventions for tackling poor air quality, and all of them have their own solution for involving citizens and raising public awareness about air quality issues. In Vantaa, the focus is on the effects of green infrastructure.[10]

1.3 URCLIM

URCLIM project aims to develop urban climate services. It is part of ERA4CS, an ERA-NET initiated by JPI Climate with co-funding of the European Union. City planners need to take into account urban meteorological effects, such as urban heat island and slippery roads and pavements, and how these effects behave in changing climate.[11] Urban climate research is highly valuable, as the population in cities is expected to grow even higher. One of the tasks for FMI's Weather Model group is to provide data on winter road conditions and on its uncertainties.

2 Theoretical background

2.1 Meteorology

2.1.1 Surface energy budget

The energy budget of the surface designates the vertical energy flux per unit area passing through the interface between air and surface. There are several physical processes involved in the energy transfer on top of the surface, but the most significant are radiative fluxes, energy fluxes related to fluid motions and energy storage and transport below the surface.[12] Here radiative fluxes consist of both solar radiation, which consist mainly of near-infrared to near-ultraviolet solar radiation, and infrared radiation emitted from clouds. These two types are commonly referred to as shortwave and longwave radiation, respectively. The surface storage is defined for a volume between the atmosphere–surface boundary and a depth where energy fluxes are negligible. For dry land, this depth is usually a few meters.[12] In the surface energy balance equation

$$\frac{\partial E_\mathrm{s}}{\partial t} =: G = R_\mathrm{s} - LE - SH - \Delta F_\mathrm{eo} \tag{1}$$

$\frac{\partial E_\mathrm{s}}{\partial t}$ or G is the surface energy storage term, R_s denotes the net radiative energy flux, LE and SH are the latent and sensible heat fluxes from surface to atmosphere, respectively, and finally ΔF_{eo} is the horizontal flux below the surface. This horizontal flux is usually small compared to other fluxes. An illustration of this can be seen in figure 1.

Daily averages of energy storage over land surfaces can be assumed to be small.[12] Therefore, equation 1 can be reformulated as

$$R_\mathrm{s} = LE + SH + \Delta F_\mathrm{eo} \tag{2}$$

Equations 1 and 2 work well on non-disturbed conditions and they are essential for any weather modeling related to surface conditions. However, some factors should be taken into account in more thorough calculations. Phase transitions of water, like

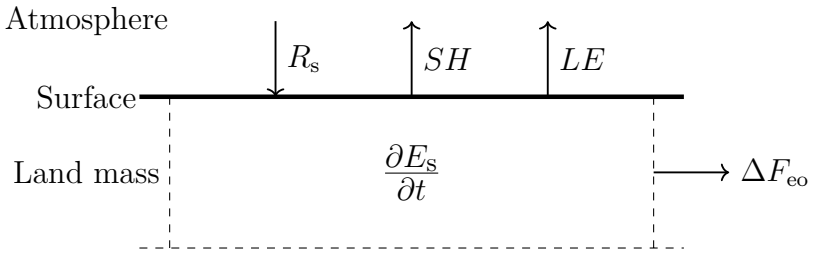

Figure 1. Surface energy balance includes surface energy storage $\frac{\partial E_s}{\partial t}$, also denoted as G, net radiative energy flux R_s, latent heat flux LE, sensible heat flux SH and ΔF_{eo}, the horizontal flux below the surface. The values are commonly measured in watts per square meter.[12]

melting of snow and ice, are at times a notable factor, as they can require 10 % of the incoming radiative energy flux [12]. Likewise, heat transfer by precipitation is an important factor when there is a temperature difference between precipitation and the surface. Factors such as chemical, biological and geothermal processes, use of nuclear or fossil fuels, and kinetic energy of the wind are not very significant for surface energy balance globally, but they can be important in local scale.[12] Furthermore, the conduction of energy inside the soil is significant when concerning the conditions above the surface, so it must be taken into account in high quality surface modelling.

2.1.2 Urban climatology

Approximately 50% of the human population is living in cities, and the number is estimated to grow even higher.[13] Although air pollution is the most notorious effect of urban areas, they impact on other climatological aspects as well.

Urban environment has a huge impact on meteorological conditions at the ground level. Air flow is affected greatly by placement of buildings and green areas, and in densely built areas direct solar radiation won't always reach the street level.[13] There are also several meteorological phenomena that are characteristic for the urban climate. One of such phenomenon is that cities are essentially warmer than the natural environment around it. The name of this phenomenon, the urban heat island, describes it well, as the city is clearly separated from its surroundings in heat and temperature maps, as seen in the figure 2. The infrastructure of the city also affects the hydrological cycle, and for example, the amount of runoff water is manifold in commercial areas when compared to rural areas.[13] This in turn affects the energy

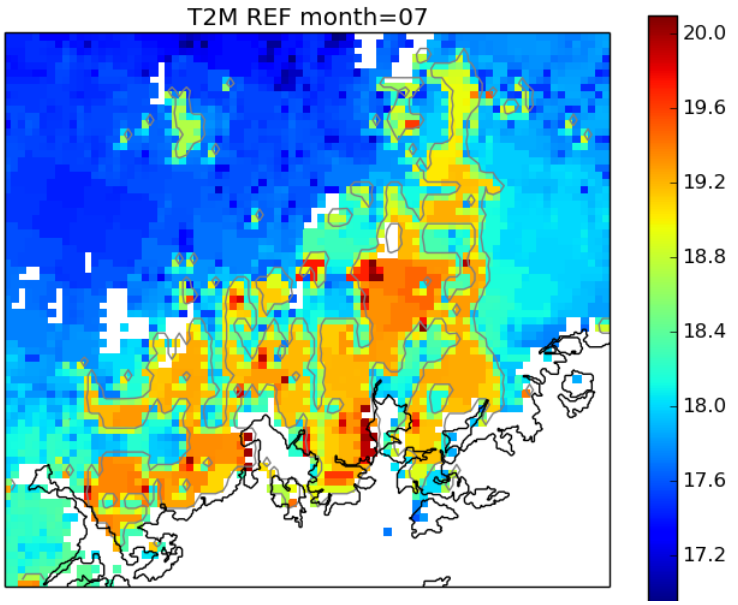

Figure 2. Monthly mean 2 m air temperature in the Helsinki capital region in July 2008. The urban heat island effect is clearly visible. The data is modelled with HARMONIE-AROME and SURFEX.

balance, as less latent heat is required to evaporate the water.

Energy balance calculations are more complex in urban environment, as there are a lot more surfaces in the form of roofs, walls and streets. Every facet does follow the surface energy balance equation (1) in principle, but because these facets are in contact with each other, they cannot be coupled separately to the atmosphere. Energy balance of urban area is therefore easier to formulate by defining a volume that covers the whole urban system. This requires that anthropogenic heat flux caused by living and working, and heat storage of the city elements are accounted for in the equation 1.[13]

In order to model urban climate, the morphology of the city must be well defined. A complete three dimensional surface with every building and tree is often too problematic to model, so the surface must be simplified. Urban canyon or street canyon is one of the methods used to simplify the surface.[13] Urban canyon is a 2-dimensional cross section of the street, in which the modelled area is represented by a single road and two buildings. They form a canyon, which has three different surfaces: road, wall and roof. These surface types and the width and the height of the canyon, that is the width of the road and the height of the buildings, define the morphology of the urban area.[13]

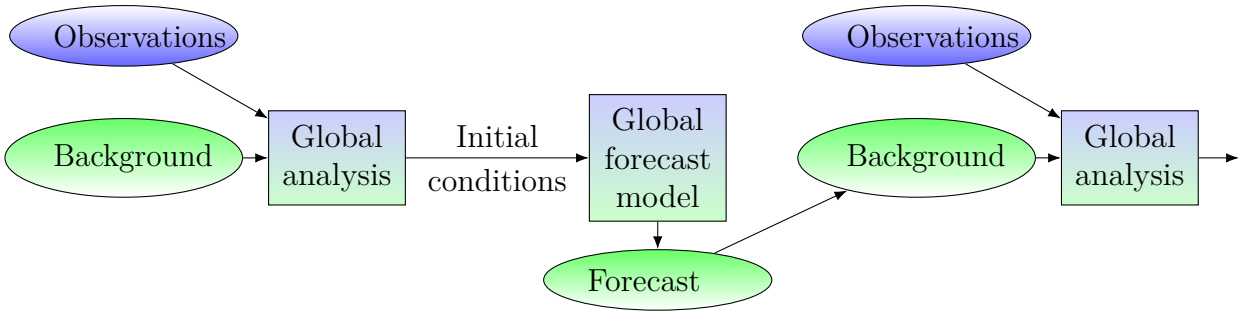

Figure 3. The cycle of data assimilation. Both observations and model forecast from the previous cycle are used to create initial conditions for the forecast model [15, p. 14].

2.2 Numerical weather prediction

Numerical weather models require well defined initial states to properly forecast the next meteorological state of the system. In addition, there can be other boundary conditions. For surface models, for example, the meteorological conditions above the surface are essential. These meteorological boundary conditions are often called forcing.[13] The physics of the models are based on the conservation of momentum, mass and energy, and for surface models on the surface energy balance equation 1.

Modern operational weather models provide forecasts for both small and large areas, the horizontal resolution ranging from one to tens of kilometers. Depending on the model and the need, the forecast can be daily short range prediction or longer, seasonal forecast.[14] Research and development of numerical weather prediction (NWP) models have resulted in longer forecasts, as every ten years the range of short range forecast has increased one day for several decades.[14] NWP has advanced considerably with the introduction of method called data assimilation.

In data assimilation, both observations and prior forecasts are used as boundary conditions for the current analysis, as seen in figure 3. Measurement stations can't observe the whole target area, so the forecast is used to cover the unobserved areas.[15] The atmosphere is modelled over space and time, and therefore the method is sometimes referred to as the four-dimensional data assimilation.[14, 16] Uncertainty of the initial state is more dominant the longer the forecast predicts, and therefore the information on the uncertainty of the prior forecasts is used to create ensemble forecasts.[14]

The development of supercomputers has also been crucial, as the models require huge amount of computational power. At the European Centre for Medium-Range Weather Forecasts (ECMWF), some of the most powerful supercomputers are used to calculate tens of billions of grid-column calculations daily.[14] Still, the lack of even more high-powered facilities is the biggest obstacle for future's forecasting in finer grids.[14]

2.3 Climate change models and RCP-trajectories

Representative Concentration Pathways (RCPs) are projections of atmospheric greenhouse gas concentrations. They were chosen from a large number of similar scenarios to represent the time-dependency of the concentrations in the changing climate.[17] There are four RCP scenarios: RCP8.5, RCP6, RCP4.5 and RCP2.6. The naming of the scenarios is based on the estimated total radiative forcing (W/m^2) in the end of the 21st century. The CO_2 concentrations and radiative forcings of the four scenarios can be seen in figures 4a and 4b, respectively.

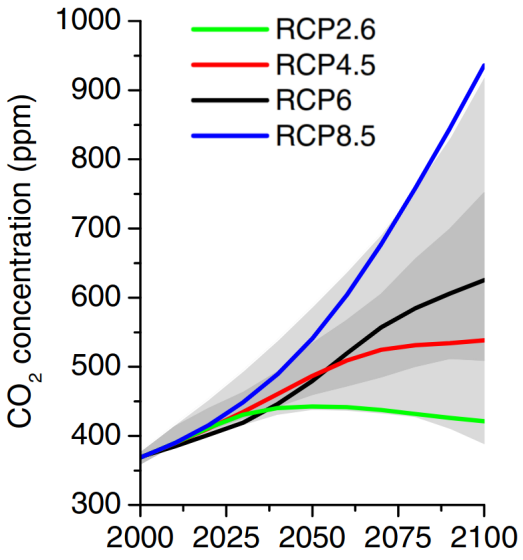

(a) CO_2 concentrations through the 21st century predicted by different RCP-trajectories.[18]

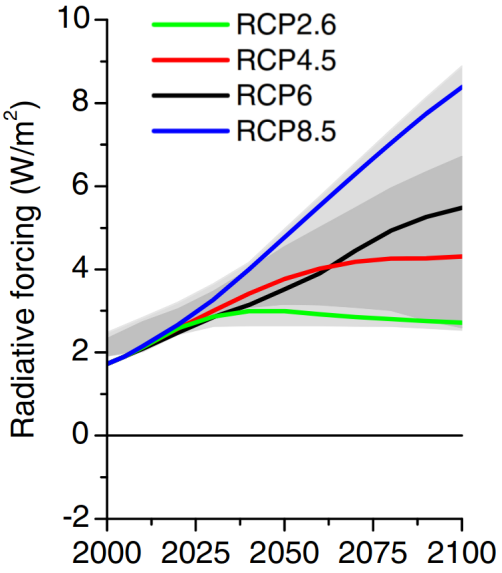

(b) Radiative forcings based on greenhouse gas predictions of different RCP-trajectories.[18]

Figure 4. RCP-trajectories predict the greenhouse gas concentrations and radiative forcing in the course of the 21st century. The dark and light grey areas indicate the 98th and 90th percentile ranges, respectively, given by the literature.[19] The figures are from the article by van Vuuren et al. (2011).[18]

RCP8.5 is 'the worst case scenario', representing the highest projected concentrations for green house gases and the highest radiative forcing. It is the only trajectory that doesn't predict any decrease in carbon emissions during the 21st century.[17] RCP6 and RCP4.5 are the intermediate pathways, both reaching stabilization in 2100-2150. The RCP2.6, sometimes called RCP3-PD, reaches a peak in radiative forcing level in the middle of the 21st century. After reaching radiative forcing of about 3 W/m^2, it starts to decrease.[17]

In a study by Kimmo Ruosteenoja, Kirsti Jylhä and Matti Kämäräinen (2016) [20], changes based on the RCP trajectories were calculated for climatological variables such as air temperature, solar radiation and precipitation in Finland. 28 climate change models were used to calculate these changes for RCP4.5 and RCP8.5 scenarios. For RCP6 the number of models used was 15, and 21 for RCP2.6.[20] A similar study was previously conducted by Kirsti Jylhä et al. (2011) [21] to estimate the effects of climate change on building energy demand in Vantaa, Jyväskylä and Sodankylä.

3 Models

3.1 RoadSurf

FMI's road weather model RoadSurf has been developed for modeling road properties, specifically road temperature and road condition.[22] The model is an energy balance model, meaning that it predicts the road conditions, e.g. road temperature and friction, based on energy fluxes at the surface using the surface energy balance equation 1. For this calculation, air temperature, wind speed, short and longwave radiation and precipitation are used as forcing. In addition to atmospheric properties, traffic is also factored in. The model takes the road maintenance into account only if a threshold snow depth is exceeded. This threshold can be adjusted and in this study it was set to 100 cm. The hydrological state of the surfaces is modelled by including hydrological processes, such as freezing and melting, into the parametrization. [22] An illustration of all the factors taken into account is shown in the figure 5.

The model calculates an index for surface condition, and it is divided into 8 categories: dry, damp, wet, wet snow, frost, partly icy, icy and dry snow. They are denoted with numbers from 1 to 8, respectively. Also, a separate categorization is determined for traffic, using surface condition and weather circumstance. Traffic index values 1, 2 and 3 corresponds to normal, difficult and very difficult condition, respectively. The indexes and their explanations can be seen in tables 1 and 2.

In operational use the model consists of two parts: the observational and the forecast-based part. In the observational part, input data is from measurements and observations. It is used as initialization for the forecast-based part. The input for the forecast-based part is from a forecast model.

The pedestrian weather model is a specific version of RoadSurf, which simulates pavement conditions in a same way that RoadSurf simulates road conditions. Difficult conditions for pedestrians don't necessary appear in the same situations as difficult traffic conditions.[2] Therefore, the calculation of pedestrian condition index differs from traffic index's one, and has more possible values. The index varies from 1 to 5, and the conditions are shown in the table 3. A pedestrian condition warning is given

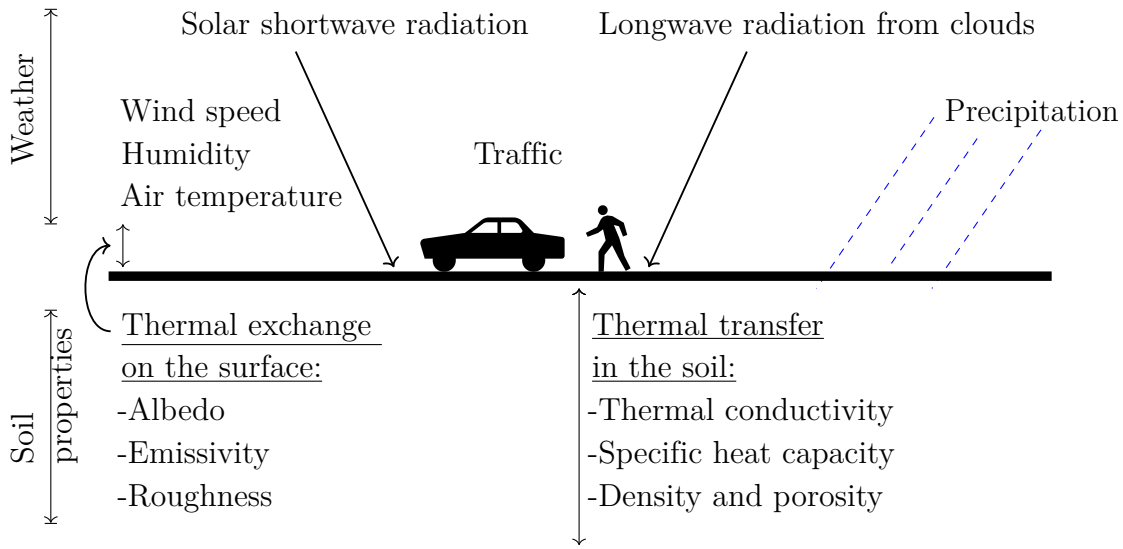

Figure 5. Many factors are taken into account in the RoadSurf. The wearing of snow and ice on top of the surface is handled differently depending on what version of RoadSurf is used. This figure is based on a similar figure in the report by Reija Ruuhela et al. (2005) [23].

Table 1. RoadSurf surface condition index explanations

Index number	Index explanation
1	Dry
2	Damp
3	Wet
4	Wet snow
5	Frost
6	Partly icy
7	Icy
8	Dry snow

Table 2. RoadSurf traffic condition index explanations

Index number	Index explanation
1	Normal
2	Difficult
3	Very difficult

Table 3. Pedestrian condition index explanations

Index number	Index explanation
1	Normal
2	Slipperiness (notice and check conditions)
3	Slipperiness due to ploughing or packing
4	Water and ice (warning)
5	Snow and ice (warning)

with index values 4 and 5. In addition, traffic and the wearing of snow, water and ice on the surface is handled differently in the pedestrian weather model. Otherwise, the basic physics are the same in both models.[24]

3.2 SURFEX and TEB

Land and ocean surface platform SURFEX is used to model air-surface interactions and surface fluxes on four surface types. These types are nature, town, inland water and ocean.[25] The model can simulate fluxes of momentum, heat, water, carbon dioxide and snow particles, among other variables. SURFEX can be run in offline mode with atmospheric forcing data or coupled to an atmospheric model. The length of the simulation can vary. The platform is designed so that it is relatively easy to implement new technical and scientific features, such as new models.[25]

TEB (Town Energy Budget) model is one of the models implemented to SURFEX. The model simulates turbulent fluxes in urban environments using the urban canyon method.[26] TEB's canyon parameters are average values from 500 m times 500 m areas, and the data is from ECOCLIMAP II, a database covering the land use over Europe.[27] The database has different covers for rural and for urban areas, such as commercial areas, airports are several different sub-urban types. Different covers in the Helsinki capital region can be seen in figure 6. These covers have different properties, such as building density and garden fraction.

Some of the urban parameters over the capital area of Helsinki can be seen in figure 7. Fraction of town (figure 7e) is the fraction of urban area in the grid point, and building fraction (figure 7a) is the building density inside this urban area. This means that the best measure for the building density of the whole area is the multiplication of these two parameters (figure 7f). These parameters are based on the different covers in ECOCLIMAP II.

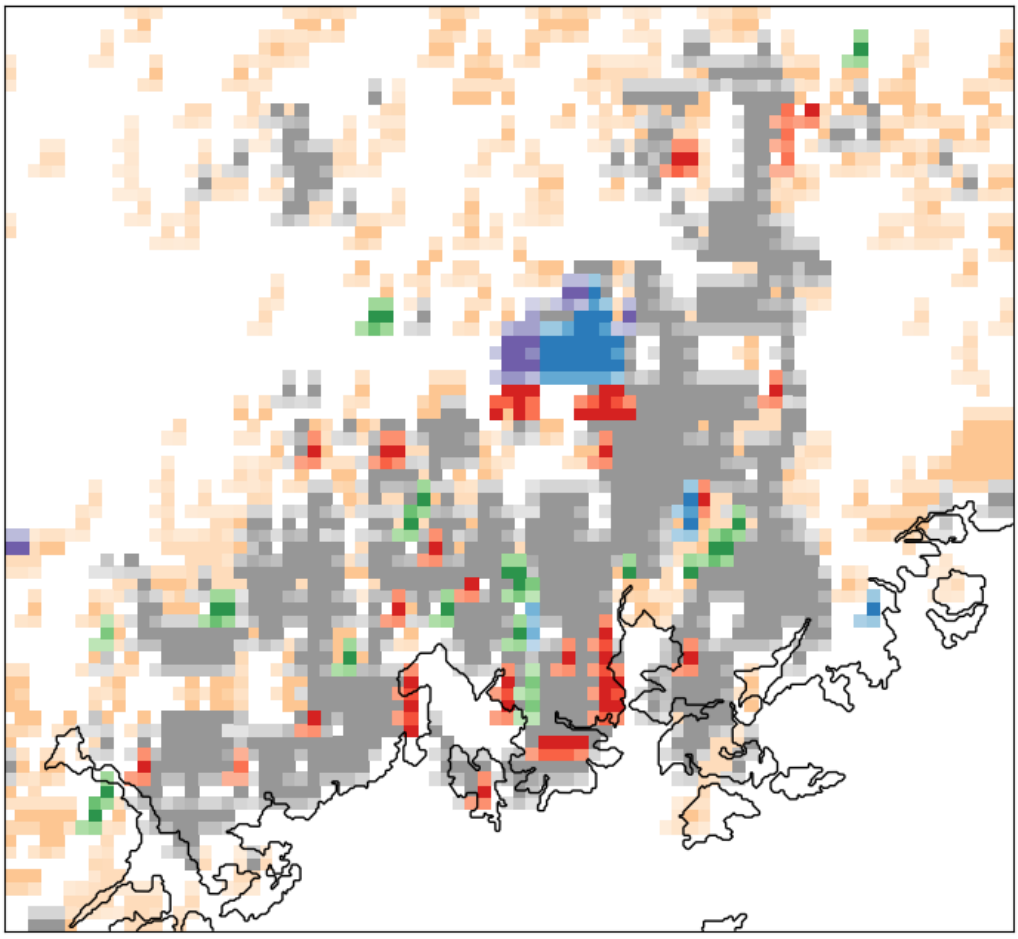

Figure 6. Different urban covers in the Helsinki capital area. Suburban areas are shown in grey, commercial and industrial areas in red; ports, airports and railroad networks in blue, parks and sport facilities in green and mineral extraction cites in purple. Rural areas with low urban fraction are shown in light orange and areas with no urban areas in white.

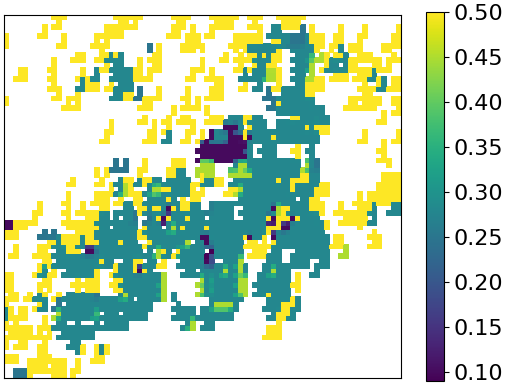

(a) Building fraction

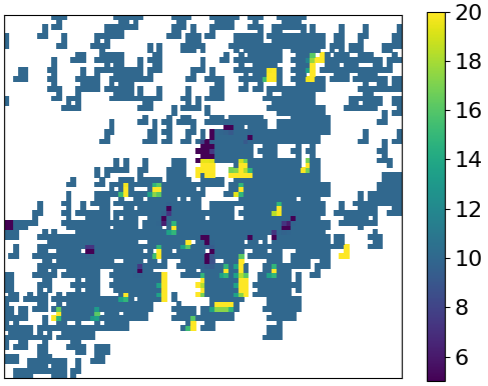

(b) Building height (m)

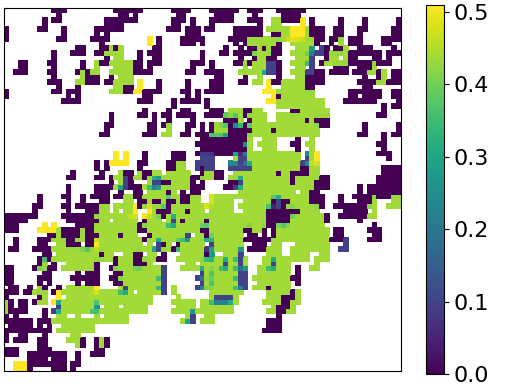

(c) Garden fraction

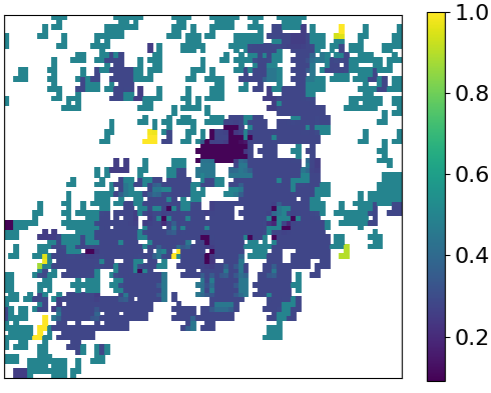

(d) Wall–plan area –relation

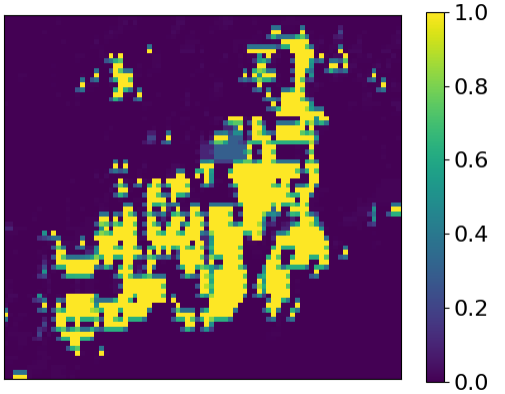

(e) Fraction of town

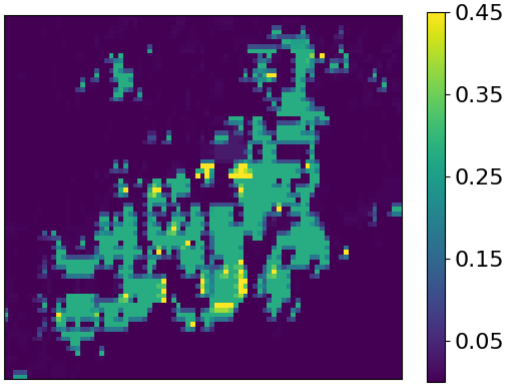

(f) Fraction of town multiplied by building fraction

Figure 7. Different urban parameters in the capital area of Helsinki. White areas are masked in TEB, meaning that there are no urban areas according to the model.

3.3 HARMONIE-AROME

HARMONIE-AROME numerical weather prediction model is in operational use in FMI's weather services. It is a configuration of ALADIN-HIRLAM system. The model uses a grid of 2.5 km, which is a typical grid size for short range operational weather models, and has 65 vertical modeling layers across the atmosphere.[28, 29] HARMONIE-AROME, like most NWP models, simulates the actual meteorological and physical processes in order to model the weather in hourly basis. In operational use, weather forecasts are made four times a day, at 00, 06, 12 and 18 UTC, and each forecast has a length of 66 hours.[29] A more profound description of the model can be found in the article *The HARMONIE-AROME model configuration in the ALADIN-HIRLAM NWP system* by Lisa Bengtsson et al. (2017) [28].

4 Methods

4.1 Test-year

The test-year used in this paper is called TRY2012. It is a representative year for recent climate, and it was created for FRAME-project (Future Envelope Assemblies and HVAC Solutions, [30]). The test-year was originally used as a reference year in the field of building engineering physics. The weather has a significant effect on buildings, especially considering dampness and water damages, and therefore a representative year was needed to analyze the effects of the weather.[21]

The test-year was constructed by selecting 12 months from years 1980–2009. Each month was selected so that the cumulative frequency distributions of daily averages of significant weather conditions were as close as possible to their respective climatological cumulative frequency distributions over the 30-year period. In other words, the distributions for January were calculated from all Januaries, and the one resembling the overall distributions the most was selected. This was done for all months separately. The daily average distributions of air temperature, humidity, solar radiation and wind speed were considered when determining the representing months. TRY2012 was calculated for different locations in Finland, and the one used here is for Vantaa.[21] The years corresponding to each month can be seen in table 4.

Hourly data is used, so that the data contains diurnal variation. This means that continuous variables, like temperature, will have a discontinuity between the last and the first hour when a month changes. For snowfall and rain there is no problem, as there can be large differences in hourly basis in the precipitation. The same goes for wind parameters. Although longwave and shortwave radiations are continuous variables, the problem is minimal. This is due to the fact that the month changes to the next at midnight, when solar radiation is zero or close to zero. Therefore, the problem is significant only for temperature and relative humidity. [21, p. 34] Discontinuities, however, will be overlooked in this paper, as only statistical results will be analyzed. HARMONIE-AROME has an appropriate initialization phase for each month, meaning that the forcing-data shouldn't behave badly. In

addition, SURFEX has storage parameters for different surface conditions, meaning that sudden changes in input files will be smoothed.

Table 4. TRY2012 test-year months for Vantaa

January	February	March	April	May	June
1990	1998	1994	2009	2006	2005
July	August	September	October	November	December
2008	2003	1997	1981	1989	1998

4.2 Model chain

Each month's HARMONIE-AROME simulation was done separately, and each month had 24 hours of initialization period. The NWP model was run only for the test-year. The output of the model was used as forcing for SURFEX, as seen in figure 8. The output had to be projected from the HARMONIE-AROME's 2.5 km grid to finer one used by SURFEX. In the case of the future climate, changes discussed in section 4.3 were applied to forcing data.

SURFEX/TEB was run in a grid of 83 x 76 separate grid points, one point corresponding to an area of 500 m times 500 m. The total area covered the whole Helsinki capital region, including Helsinki, Espoo and Vantaa. The grid points were independent, meaning that they weren't connected to adjacent squares, apart from the forcing data provided by HARMONIE-AROME. Some of the points were masked in TEB, as there was no town according to the database.

One year-long SURFEX/TEB simulation was done for test-year with original forcing data and another for the future climate with modified forcing data. A three-month-long initialization period was used for both cases to get appropriate starting conditions. These simulations were operated on ECMWF (European Centre for Medium-Range Weather Forecasts) supercomputer.

SURFEX/TEB output data had to be formatted to RoadSurf's input format. Temperature was changed from kelvins to Celsius degrees and relative humidity to percentage. Emissivity and albedo of the road was used to convert the absorbed longwave and shortwave radiations given by SURFEX and TEB to total received radiations. For precipitation, rain and snow forcing data from HARMONIE-AROME was used.

RoadSurf was used with 'default' settings, and the road type was set as 'normal road'. In this study, there wasn't actual observational and forecast-based parts, as the whole simulation period was modeled based on observations from the months of test-year. Therefore, the length of RoadSurf's observational phase has no significance. It was set to be two thirds of the simulation period. RoadSurf runs were performed twice, separately for road weather and pedestrian conditions.

Two modifications were made to RoadSurf's code so that the year-long simulation of the test-year could be done. The maximum simulation length was changed from a few days to 365 days. In addition, output file naming was modified so that simulation's SURFEX grid point indices would show on the file name. This was done to ease the file-processing, as there were over two and a half thousand different points which were simulated with RoadSurf.

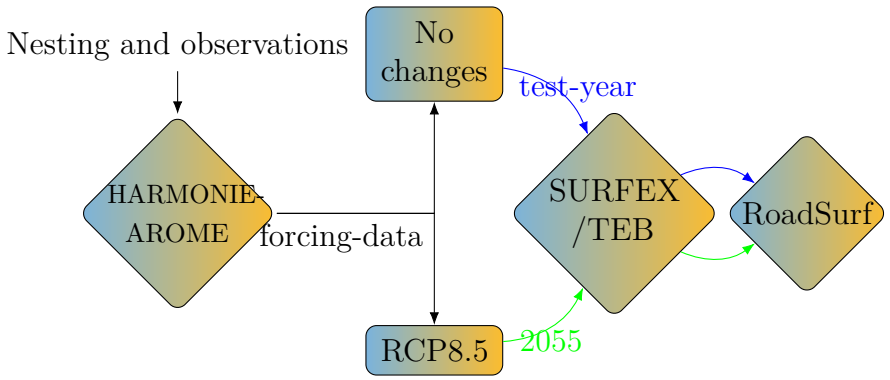

Figure 8. The model chain used in this study

4.3 Generating the future climate

Changes had to be applied to test-year's meteorological data in order to simulate the effects of climate change. The time period of 2040–2069 was selected as the future climate to be examined. This period was chosen, because it is reasonably close to present so that these results can be utilized by city and road maintenance authorities, but it is also so far away that there should be prominent effects. For the same reason, RCP8.5 was chosen as the trajectory in which the meteorological changes are based on. This future time period is later referenced as 2055, but it should be highlighted that these results won't predict the actual weather of 2055, but rather the mean values over several decades in that time period.

The effects of climate change on temperature, wind speed and direction, total precipitation and short wave radiation are based on a study by Kimmo Ruosteenoja et al. (2016) [20]. The study did not provide any data on humidity, so changes for relative humidity are based on the study by Kirsti Jylhä et al. (2011) [21]. The method used for applying the changes to the test-year's hourly meteorological data is the so-called delta change -method, where daily variation is assumed to stay similar and the changes to variables are added to the hourly weather data identically regardless of the time of the day.[21] The changes were made so that the new data would be statistically inline with the climate change models.

As SURFEX needs rain and snowfall as separate inputs, changes in these conditions must be calculated separately from total precipitation. In addition, longwave radiation data must also be calculated for 2055 climate, as the studies provided changes only for shortwave radiation.[20, 21]

Calculating changes for the different forms of precipitation isn't trivial, as the relation between snowfall and rain depends not only on the temperature at ground level, but also on the temperature profile and other weather variables as well. If the proportions of rain and snowfall would be conserved while temperature was altered, there would be snow and sleet in higher temperatures than normally. Therefore, hourly ratios between snowfall and total precipitation were calculated from the test-year data and then were plotted against temperature. A linear fit was made in the temperature range where both snowfall and rain exist, and that fit can be seen in figure 9. Based on this fit, at temperatures above 2.02 °C all total precipitation was converted to rain in 2055 climate. Likewise, below -0.52 °C all precipitation was converted to snowfall. In temperatures between -0.52 and 2.02 °C, the ratio given by the fit was used to get values for rain and snowfall.

Several methods were considered in order to produce the absent longwave radiation data for 2055 climate. Downward longwave radiation on the surface is mostly radiation emitted from clouds. Therefore it depends mostly on cloudiness, but also on air temperature and humidity as they change the emissivity of the atmosphere.[31] Cloud data for the test-year was not directly available, so temperature and humidity were the only options to determine the longwave radiation in 2055 climate. Of the two, humidity showed better linear dependency with the longwave radiation in the test-year data, although the dependency was divided into two different linear curves, as seen in figure 10a. This can be explained by cloudiness: the upper curve in figure

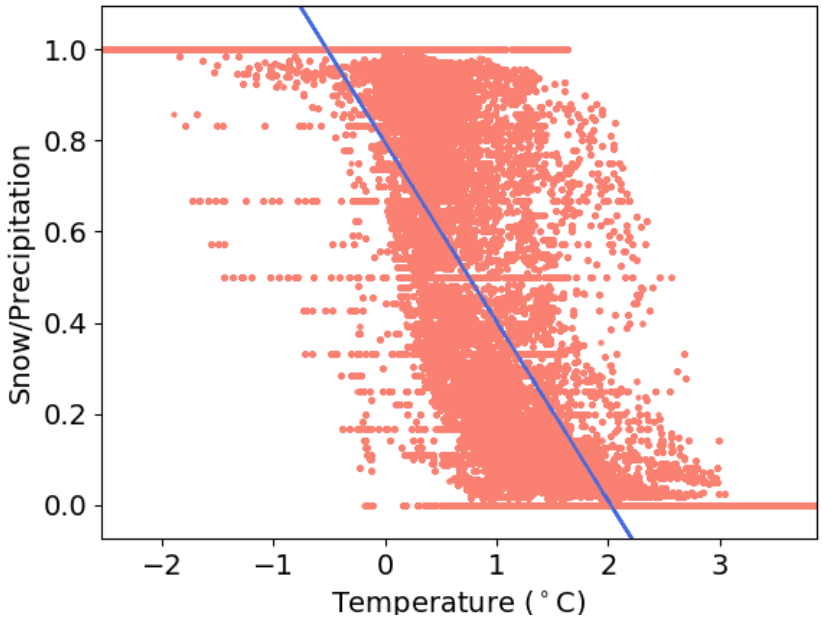

Figure 9. The proportion of snow from total precipitation is plotted against temperature. The plotted data set consists of every test-year grid point and hour which has at least 5.0 $\cdot 10^{-5}$kg/m^2/s precipitation. The linear fit is calculated from all the data points of the whole year where there are both rain and snowfall.

10a contains the cloudy hours as intensity of longwave radiation is increased, and the lower curve is for clear sky cases. The sparse points between the curves are then the partly cloudy hours, consistently with the U-shaped distributions of cloudiness. The following method was created in order to get an explicit connection between air specific humidity and longwave radiation.

For each of test-year's months, longwave radiation was plotted against humidity (figure 10a). In the figure, two quite linear curves can be seen. Data points were initially divided to two sets using linear fit to split the data. For both halves of the set, a new linear fit was formed to get representations for upper and lower curves (figure 10b). To get even more representative fits, the whole data set was again halved, this time using mean valued line calculated from the two linear fits from previous phase (figure 10c). This method was repeated several times, and after 10 iterations linear fits clearly approach a nice limit (figure 10d). The tenth iteration was therefore used to get linear fits for both upper and lower curves. Also, the last splitting line was recorded for later use.

To utilize these linear fits, longwave radiation and specific humidity was stored

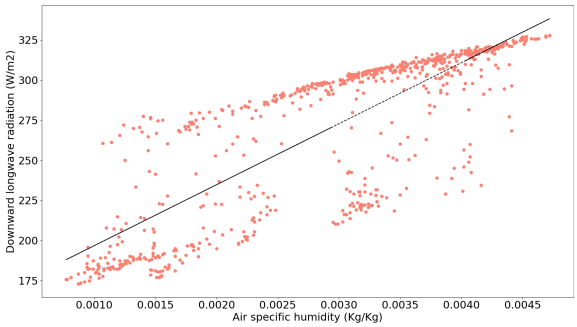

(a) A linear fit is plotted between air specific humidity and longwave radiation for all months separately. The data shown in this figure is for test-year's January.

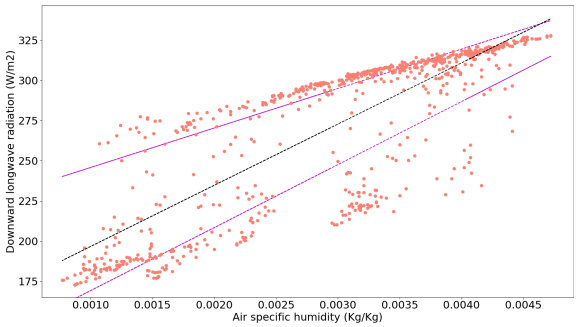

(b) The linear fit of the whole data set is used to divide the set into two subsets. New linear fits are plotted for these subsets.

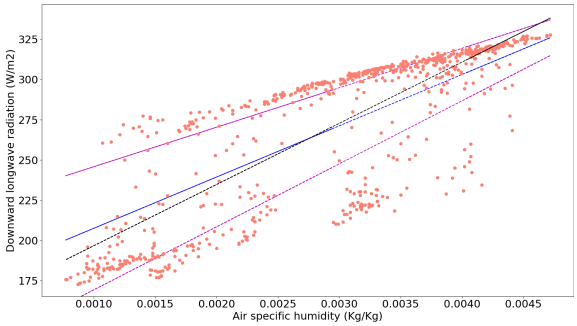

(c) A new fit is used to half the set again. This time, the fit is calculated using mean values of parameters from fits of previous subsets.

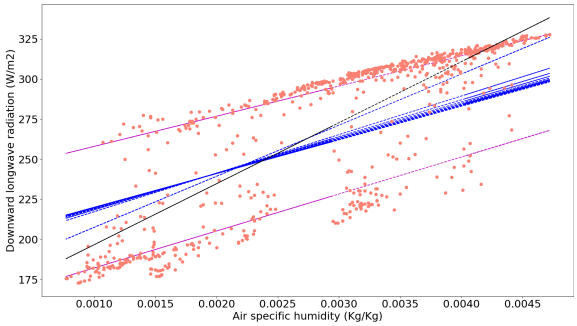

(d) After repeating the steps 10a–10c 10 times, the fits of the subsets represent quite well the two linear curves seen in the data set.

Figure 10. The process of determining longwave radiation for 2055 climate. This method was developed for this paper.

for every data point from the test-year data. Then, after calculating the changed humidity for 2055 climate, a new value for longwave radiation was calculated using the new humidity value and either the upper or lower linear fit, depending on whether the original humidity–longwave radiation –point was over or under the splitting line. In other words, every humidity–longwave radiation –point was scaled along appropriate fit based on the change in humidity. This method neglects the partly cloudy data points, as they move to the nearest fit in the 2055 climate data.

5 Results

5.1 Meteorological conditions

The monthly averages of test-year and 2055 climate forcings are presented in figure 11 (air temperature), table 5 (relative humidity and wind speed), table 6 (scattered and direct shortwave radiation) and table 7 (total shortwave and longwave radiation). The relative changes in the tables are calculated relative to the test-year data, and the values are rounded to two decimal places. The monthly total precipitation is shown in figure 12.

Table 5. Monthly mean values of relative humidity and wind speed from the test-year forcing, and the changes for the 2055 climate.

	Relative humidity			Wind speed		
Month	Test-year (%)	2055 (%)	Rel. change (%)	Test-year (m/s)	2055 (m/s)	Rel. change (%)
Jan	94.26	94.46	0.21	4.75	4.81	1.20
Feb	92.02	91.59	-0.47	5.23	5.25	0.46
Mar	89.03	87.80	-1.39	4.43	4.45	0.30
Apr	66.49	64.02	-3.73	3.85	3.88	0.86
May	52.26	50.91	-2.58	3.84	3.90	1.74
Jun	57.52	55.59	-3.35	3.87	3.91	1.05
Jul	58.11	54.98	-5.38	3.57	3.64	1.85
Aug	62.20	59.18	-4.86	3.71	3.75	1.05
Sep	67.74	65.84	-2.80	4.62	4.63	0.25
Oct	84.14	83.58	-0.67	4.05	4.06	0.45
Nov	90.44	91.17	0.81	4.19	4.26	1.73
Dec	92.80	93.59	0.84	4.65	4.70	1.25

Temperature is the most relevant of the modified forcings, and it is also affected the most by the applied changes. The models predict that the mean temperatures of January, March and December will change from below to above freezing, meaning that only February will have below freezing mean temperature. The changes in the monthly average temperatures range from 2.5 °C in May to 4.3 °C in January. The

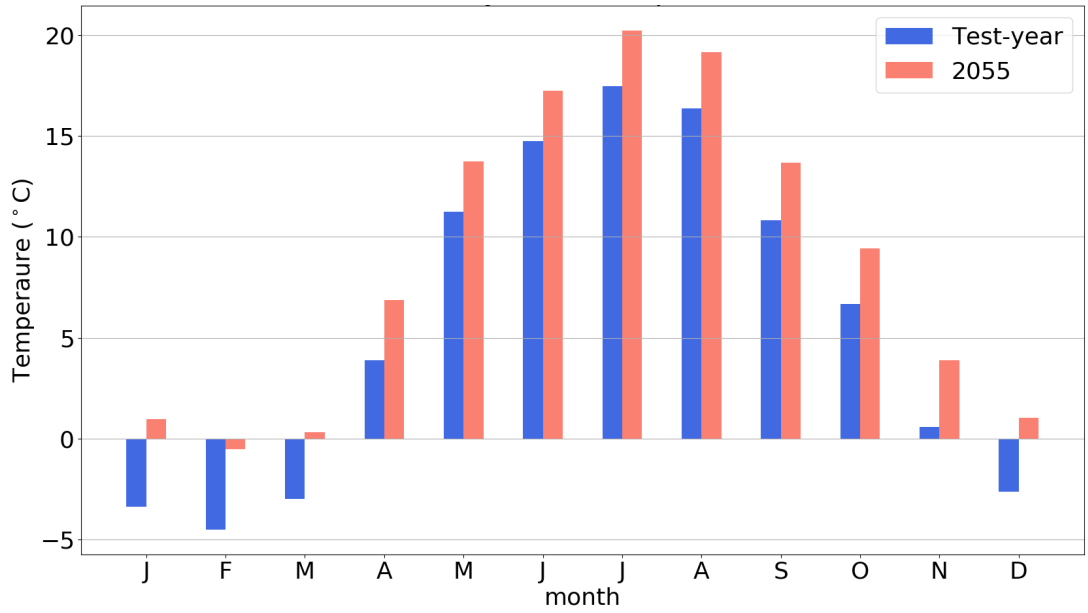

Figure 11. Monthly mean temperatures in the test-year and in the 2055 climate at the Helsinki-Vantaa airport.

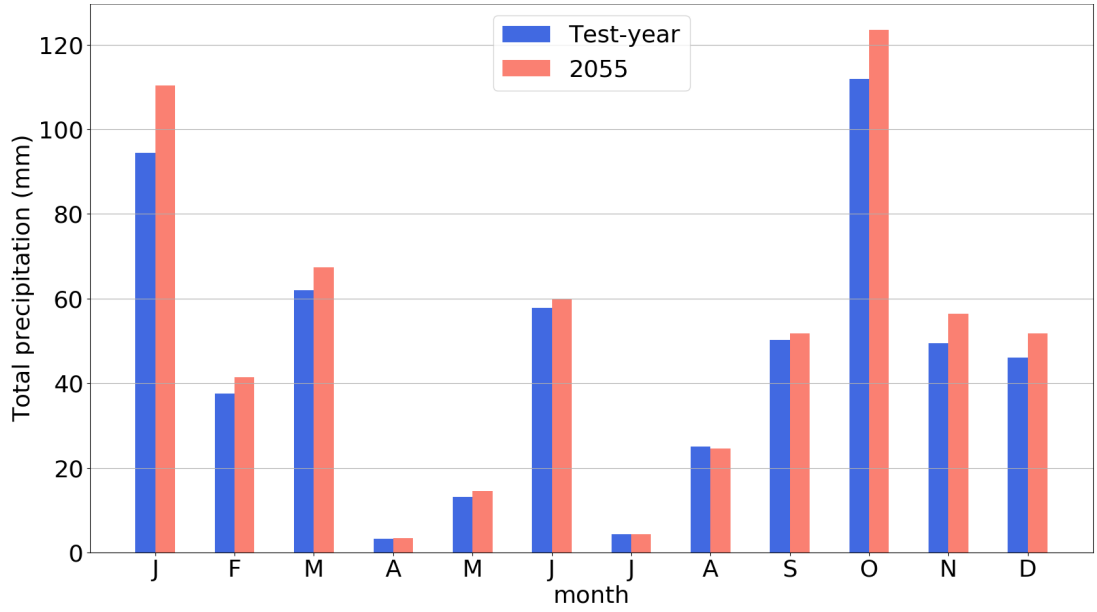

Figure 12. Monthly total precipitation in test-year and in 2055 climate at the Helsinki-Vantaa airport.

summer months have consistently smaller absolute changes, and the average monthly change is 3.1 °C. In every month the average temperature rises and thus the annual temperature cycle has a similar shape in the 2055 climate as in the recent climate.

Table 6. Monthly mean values of scattered and direct shortwave radiation from the test-year forcing, and the changes for the 2055 climate.

	Scattered shortwave radiation			Direct shortwave radiation		
Month	Test-year (W/m^2)	2055 (W/m^2)	Rel. change (%)	Test-year (W/m^2)	2055 (W/m^2)	Rel. change (%)
Jan	7.21	6.91	-4.22	2.49	1.99	-19.83
Feb	21.47	20.99	-2.25	12.94	11.04	-14.67
Mar	53.59	53.21	-0.70	40.32	37.32	-7.45
Apr	79.78	79.83	0.06	98.48	101.18	2.74
May	83.88	83.91	0.03	158.05	163.01	3.14
Jun	109.47	109.51	0.03	142.13	147.88	4.05
Jul	100.87	100.89	0.02	156.70	164.62	5.05
Aug	79.47	79.49	0.03	106.26	116.57	9.69
Sep	55.57	55.62	0.09	63.53	70.90	11.60
Oct	23.99	24.08	0.35	11.89	13.83	16.32
Nov	9.75	9.70	-0.55	3.14	2.90	-7.68
Dec	4.90	4.82	-1.53	2.30	1.96	-14.83

Changes in relative humidity are quite small. The average change in monthly mean humidity values is -1.2 percentage points. The largest relative change is in July (-5.4 %).

The average wind speed increases in every month, as seen in table 5. The largest relative change is in July (1.9 %), and the largest absolute change is in November (0.072 m/s).

Changes in direct shortwave radiation are consistently larger than the corresponding scattered shortwave radiation changes. This is due to the used method: changes in total shortwave radiation are primarily applied to direct and secondarily to scattered shortwave radiation.[21] For the same reason the changes in scattered shortwave radiation are the more dominant factor for total shortwave radiation changes the less direct shortwave there is.

The relative changes in longwave radiation are stronger in winter time, although less than 9 % in every month. The changes are not in line with relative humidity changes, which is expected, as the longwave radiation changes are based on changes in air specific humidity, not in relative humidity.

Table 7. Monthly mean values of total shortwave and longwave radiation from the test-year forcing, and the changes for the 2055 climate.

	Total shortwave radiation			Total longwave radiation		
Month	Test-year (W/m^2)	2055 (W/m^2)	Rel. change (%)	Test-year (W/m^2)	2055 (W/m^2)	Rel. change (%)
Jan	9.70	8.90	-8.22	269.80	293.11	8.64
Feb	34.41	32.02	-6.92	245.02	267.01	8.98
Mar	93.91	90.53	-3.60	245.26	265.25	8.15
Apr	178.27	181.01	1.54	263.02	280.45	6.63
May	241.93	246.91	2.06	290.89	302.05	3.84
Jun	251.60	257.38	2.30	321.06	333.28	3.81
Jul	257.58	265.51	3.08	332.15	341.83	2.91
Aug	185.73	196.06	5.56	335.60	348.06	3.71
Sep	119.10	126.52	6.23	301.79	315.66	4.60
Oct	35.88	37.90	5.64	313.38	329.88	5.26
Nov	12.89	12.60	-2.29	278.77	301.40	8.12
Dec	7.20	6.78	-5.78	257.10	279.47	8.70

5.2 Surface conditions

As the interest of this study is mainly in wintertime conditions, only months from October to April are addressed later on, and these months are collectively referred to as winter or winter months. The fractions of different surface conditions in winters of test-year and 2055 climate are shown in figure 13.

The figure 13 shows that 'dry' and 'damp' conditions increase significantly (13.1 % and 3.8 %, respectively) when shifting to 2055 climate, while 'wet' and 'wet snow' conditions increase only slightly (0.6 % and 0.2 %, respectively). Proportions of 'frost', 'partly icy', 'icy' and 'dry snow' conditions diminish significantly, as they decrease by 6.1, 4.5, 2.4 and 4.8 percentage points, respectively.

The increases in conditions related to wetness ('wet', 'damp' and 'wet snow') can be related to two things. First, the increased precipitation seen in figure 12 of course increases the amount of water in the ground. Second, the risen temperatures (figure 11) reduce the amount of snow by melting it to water. The increase in 'dry' condition may relate to the fact that water-related conditions, such as 'wet', are not as long-term as snow-related conditions.

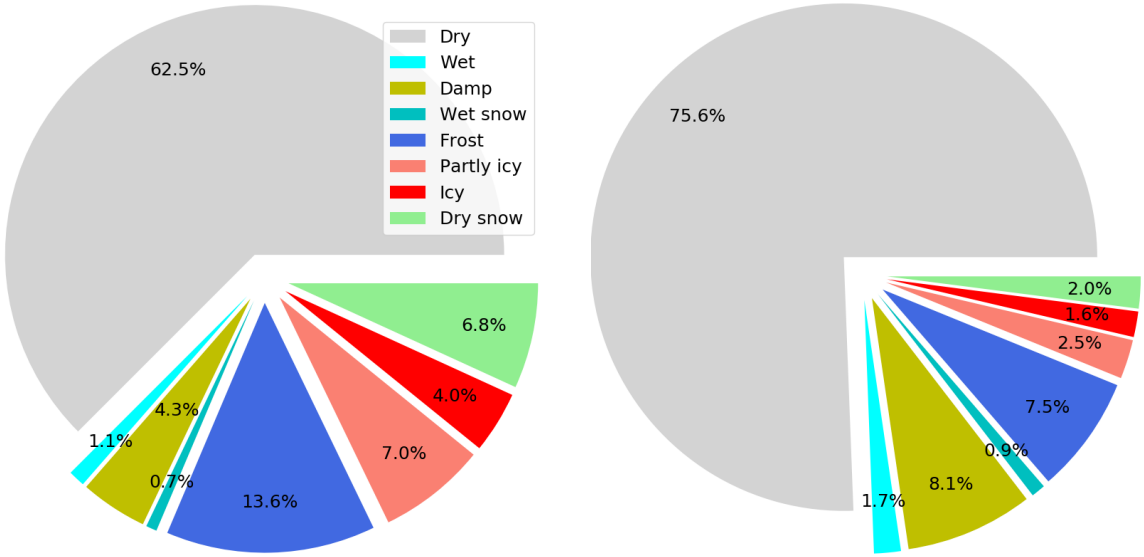

(a) Test-year winter. **(b)** 2055 winter.

Figure 13. Wintertime surface condition proportions in different climates. The charts contain data from October to April.

5.2.1 Traffic conditions

The occurrences of difficult or very difficult traffic conditions on each month for both test-year and 2055 are shown in figure 14. The spatial variation of difficult and very difficult traffic conditions on test-year winter and the spatial variation of the changes when compared to 2055 climate are shown in figure 15.

The average number of hours when traffic condition is difficult or very difficult decreases considerably in every month, as seen in figure 14. In 2055 climate, December still has the most difficult or very difficult traffic conditions. An interest notion is that January, February and March have similar amounts of difficult traffic condition hours in the 2055 climate, unlike in the test-year case where January has over 80 difficult traffic condition hours more than February or March. The models predict that the total number of difficult or very difficult traffic condition hours in a year drops 52 % when moving from recent climate to 2055 climate.

Figures 15a and 15b show that difficult traffic conditions are not affected by urban covers. Although the figures show difference between the suburban and surrounding rural areas, the results of the rural areas are not reliable. The urban fraction in the rural area is only few percentage, while the BLD-fraction is very high, 0.5. Therefore, these covers are not necessary describing the areas realistically.

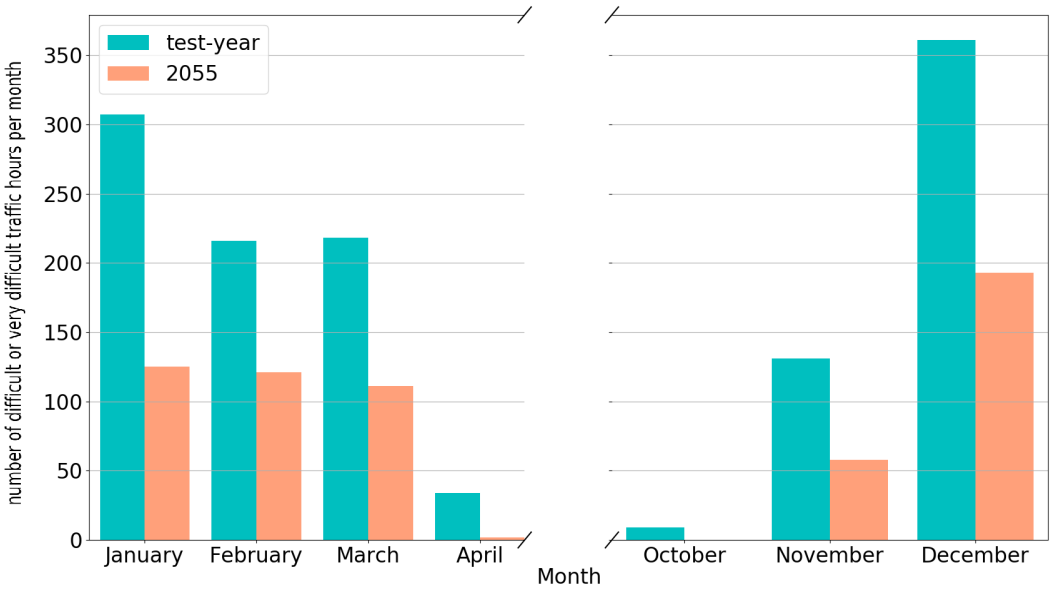

Figure 14. Monthly mean number of difficult or very difficult traffic condition hours in test-year and in 2055 climate.

Figure 15c shows that very difficult traffic conditions are more likely in parks and sport facilities and also in the airport. There are also coastal areas which seem to be more vulnerable to these conditions, but this can also be caused by isolated weather phenomena. The concentrations in parks etc. are less likely to be caused by such phenomena, as the areas are smaller than the 2.5 x 2.5 km grid size used by HARMONIE-AROME. The figure 15d shows that the changes are stronger in areas where the original number of very difficult conditions are more common. There are areas with negligible increases.

5.2.2 Pedestrian conditions

Monthly mean number of instances of different pedestrian conditions for both test-year and 2055 climate months can be seen in figure 16. Different pedestrian conditions in test-year and the 2055 changes are shown on map in figures 17 and 18.

Most of the different pedestrian conditions occur significantly less in the 2055 climate than in the recent climate, as seen in figure 16. 'Slipperiness' decreases in every month, and the biggest drop is in January with a 60 hours decrease. 'Slipperiness due to ploughing or packing' decreases in every month except in February and December,

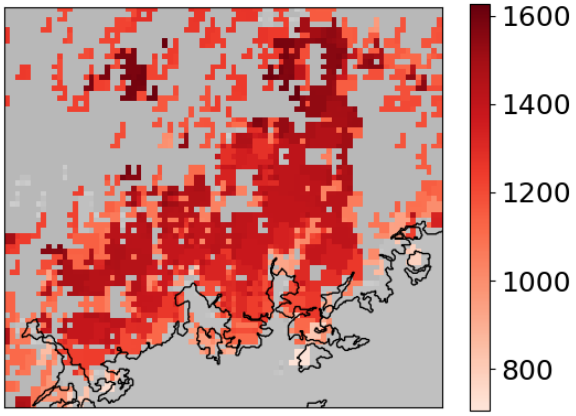

(a) Number of hours when traffic condition is 'difficult' on test-year winter.

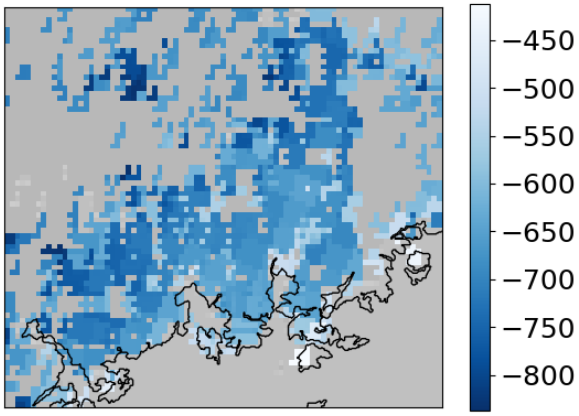

(b) The difference in number of hours that traffic condition is 'difficult' between test-year and 2055 winter.

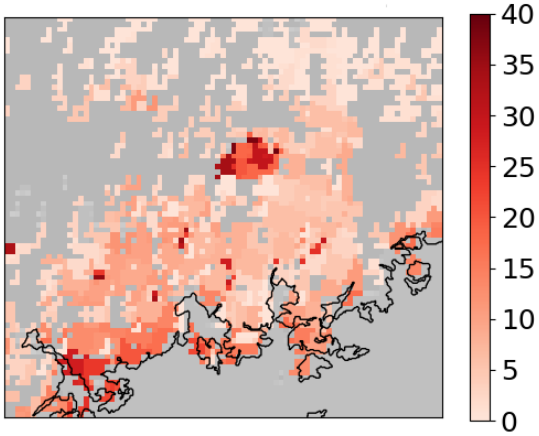

(c) Number of hours when traffic condition is 'very difficult' on test-year winter.

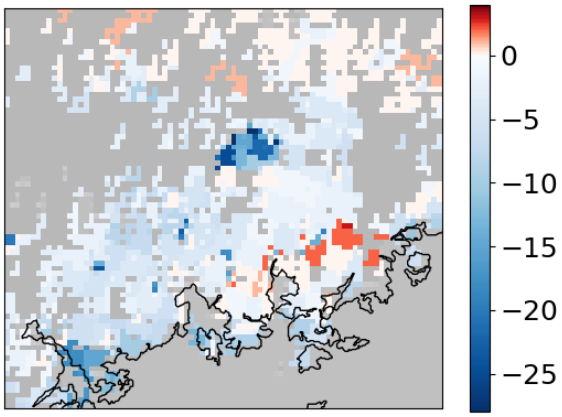

(d) The difference in number of hours that traffic condition is 'very difficult' between test-year and 2055 winter.

Figure 15. Changes on traffic index based on RCP8.5 scenario in the Helsinki capital region. Masked grid points are shown in grey. Maps contain data for all wintertime months, from October to April.

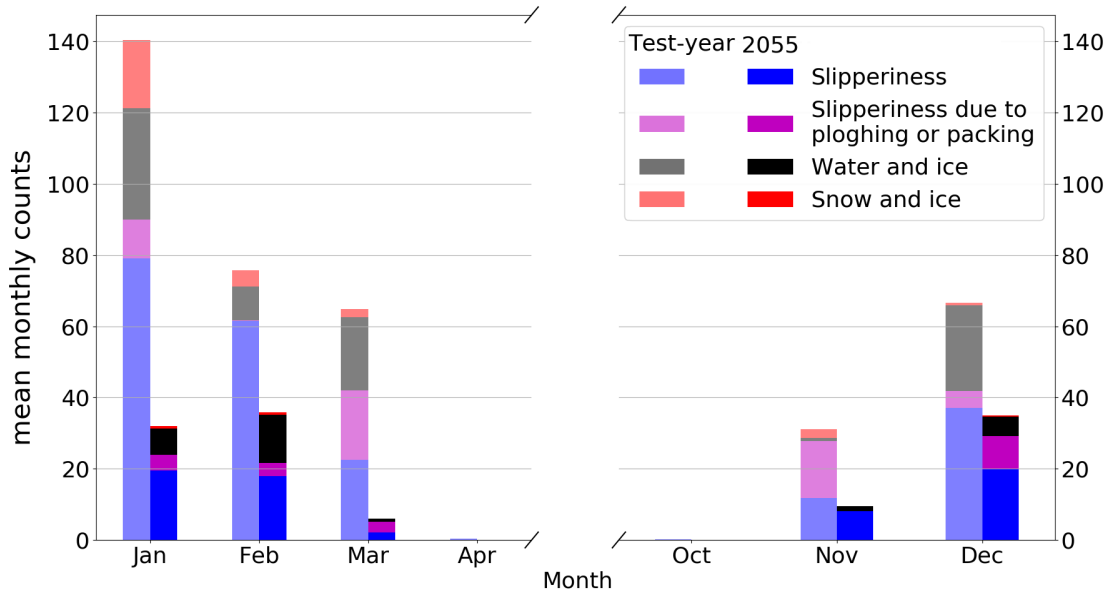

Figure 16. Monthly mean of pedestrian indexes for test-year and for 2055 climate.

where the amount increases in average by 3.6 and 4.5 hours, respectively. The number of 'water and ice' cases decrease significantly in every month except in February and November, where there are slight increases (4.0 and 0.4 hours, respectively). The number of 'snow and ice' cases decrease significantly throughout the year, as the average total annual amount of these cases drop from 29.2 hours to 1.7 hours.

According to the models, 'slipperiness' is more common in commercial and industrial areas than in other urban types in recent past climate and less common near the sea, as seen in figure 17a. The annual amount of 'slipperiness' cases also decreases more in commercial and industrial areas (figure 17b). The number of 'slipperiness due to ploughing or packing' cases seem to depend mainly on the distance to the sea (figure 17c), as does the change when comparing to the 2055 climate (figure 17d). 'Water and ice' cases seem to be more common in commercial and industrial areas, but the figure 18 shows that both the number of 'water and ice' and 'snow and ice' cases have also some local variation not related to urban covers. These variations could be caused by some isolated meteorological phenomena, such as a heavy snowstorm on a small area, in which case these results don't represent the spatial variation of these conditions that well.

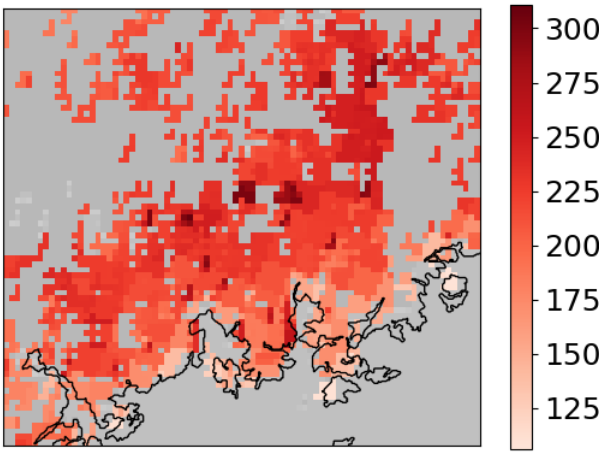

(a) Number of hours that pedestrian conditions are slippery on test-year winter.

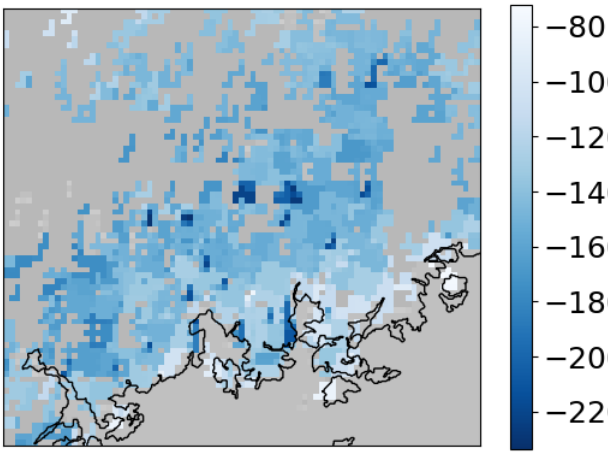

(b) The difference in number of hours that pedestrian conditions are slippery between test-year and 2055 winter.

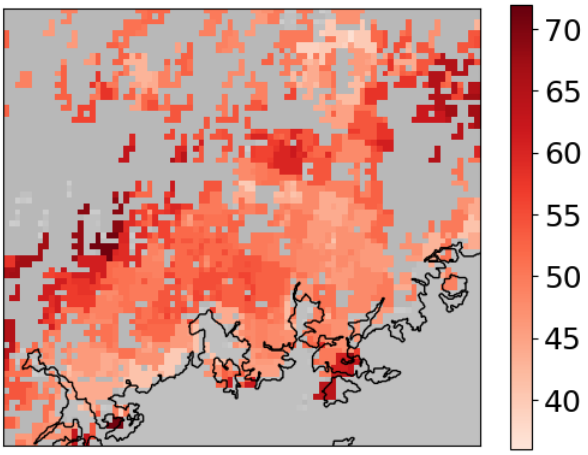

(c) Number of hours that pedestrian conditions are slippery due to ploughing or packing on test-year winter.

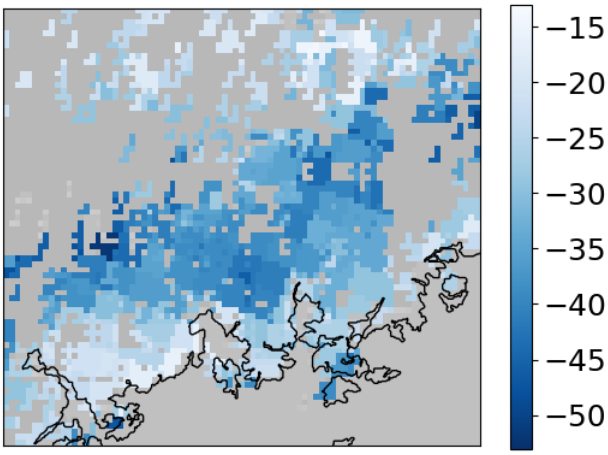

(d) The difference in number of hours that pedestrian conditions are slippery due to ploughing or packing between test-year and 2055 winter.

Figure 17. Changes on pedestrian condition indexes 2 and 3 based on RCP8.5 scenario in the Helsinki capital region. Masked grid points and grid points with water elements are shown grey. Maps contain data for all wintertime months, from October to April.

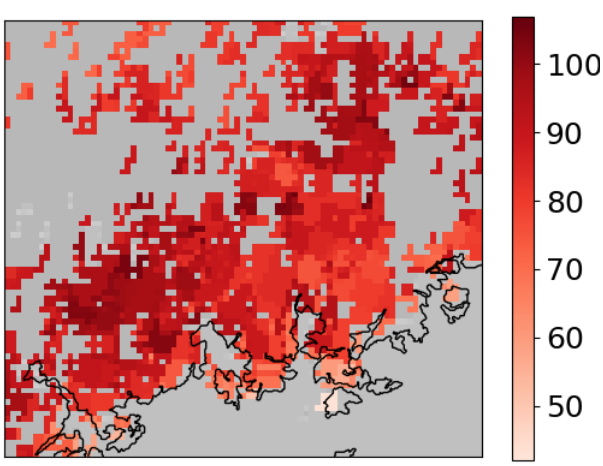

(a) Number of hours that pedestrian condition is 'water and ice' on test-year winter.

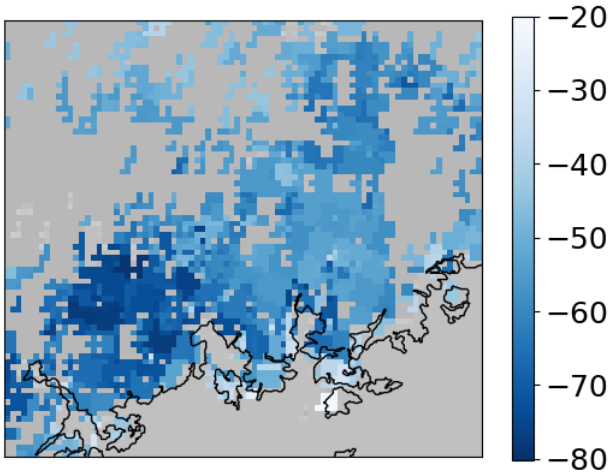

(b) The difference in number of hours that pedestrian condition is 'water and ice' between test-year and 2055 winter.

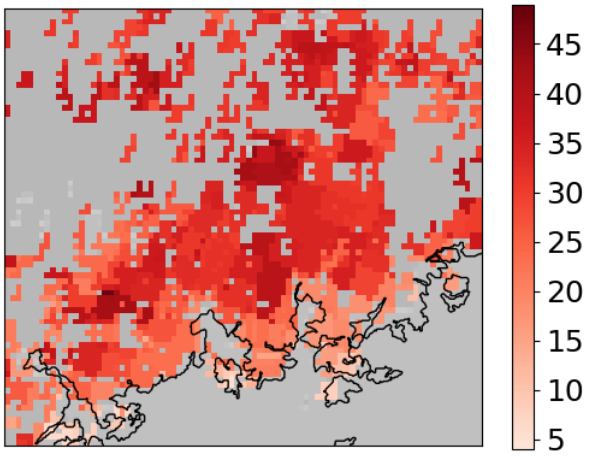

(c) Number of hours that pedestrian condition is 'snow and ice' on test-year winter.

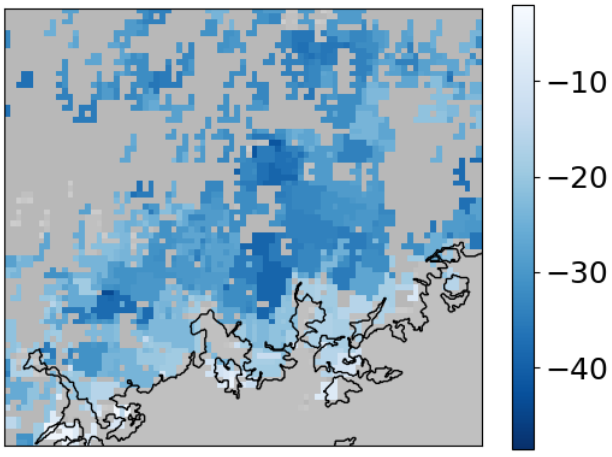

(d) The difference in number of hours that pedestrian condition is 'snow and ice' between test-year and 2055 winter.

Figure 18. Changes on pedestrian condition indexes 4 and 5 based on RCP8.5 scenario in the Helsinki capital region. Masked grid points and grid points with water elements are shown in grey. Maps contain data for all wintertime months, from October to April.

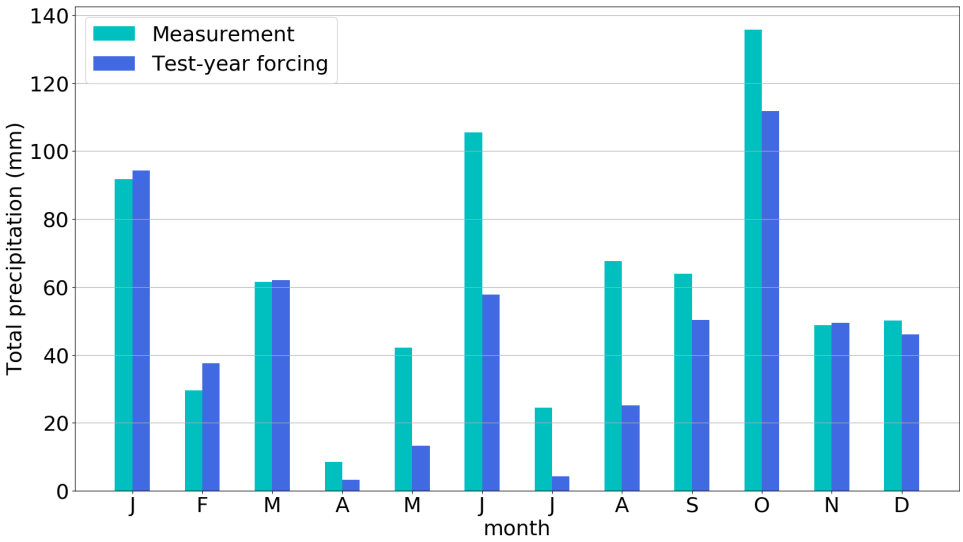

Figure 19. Monthly total precipitation for observations in Helsinki-Vantaa airport and for the forcing data of the test-year.

5.3 Verification

The simulated test-year weather data was verified using observations from Helsinki-Vantaa airport. The simulated data was compared to the observations made in the actual months of the test-year (table 4). To verify the model chain, the same models were used to model the winter 2014–2015, and these results were compared to observations from a road weather station in Jakomäki.

The figure 19 shows the monthly total precipitation of the simulated test-year months and observed precipitation in the corresponding months. The model shows much less precipitation during the summer than it should. This may be caused by too short modeling times (6-hour-periods). Apart from the summer months, the precipitation is modelled well.

Diurnal variation of observations and simulated weather parameters in winter months is presented in the figure 20. The shown measurement values are averages calculated from 3-hour data measured in December 1998, January 1990 and February 1998, and the simulated data is test-year hour-data from SURFEX for December, January and February.

The midday peak in diurnal variation of winter temperature seems to be modelled quite nicely as seen in the figure 20a, but evening, night and early morning has almost 1 °C too cold temperatures. The simulated relative humidity differs from the observed values 6-8 percentage points during the whole diurnal cycle, but the shapes

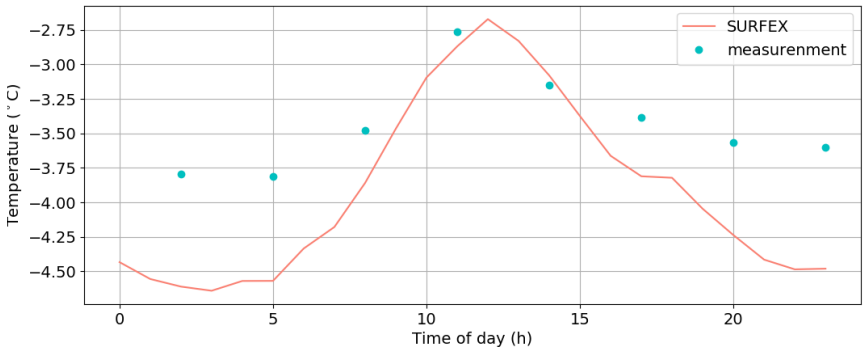

(a) Winter daily temperature variation

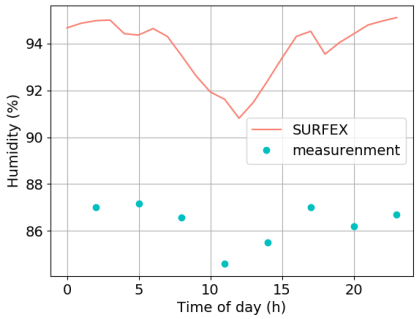

(b) Winter daily humidity variation

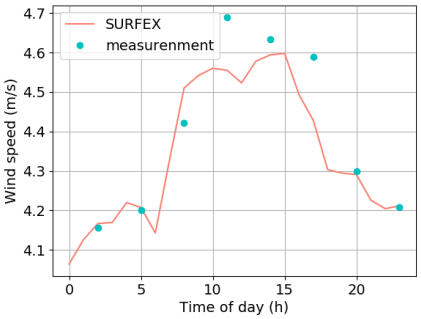

(c) Winter daily wind speed variation

Figure 20. The mean diurnal variation of temperature, humidity and wind speed for winter months (December, January and February).

of the humidity variations are similar. The wintertime wind speed is modelled very well, as the diurnal cycle of simulated data follows the observations almost identically, although the wind speed is a little too weak in midday.

The surface temperature comparison between road weather station measurement in Jakomäki and modelled data from SURFEX and RoadSurf can be seen in the figure 21. It can be seen that both models follow the observations pretty well, but SURFEX predicts couple degrees too low temperatures for the lowest temperatures. RoadSurf seems to predict the surface temperature very well throughout the simulated period.

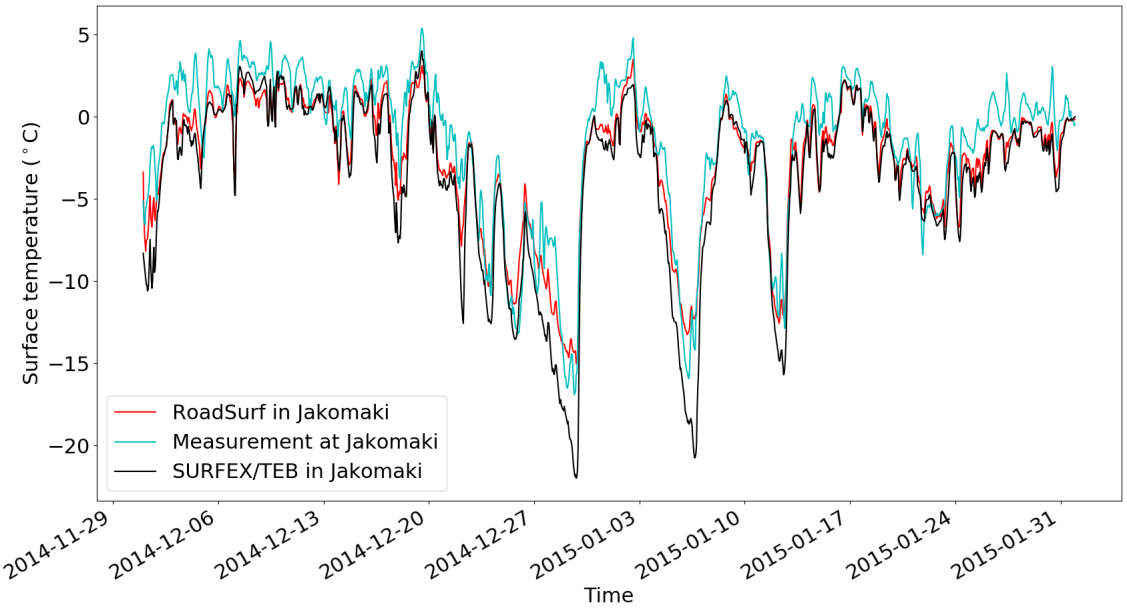

Figure 21. Comparison between observed surface temperature, and modelled surface temperature from SURFEX and from RoadSurf.

6 Conclusion

The test-year is a suitable tool to assess the climate in statistical way, while containing the daily and hourly variability in meteorological data. As this variation is essential for changes in difficult road and pedestrian conditions, the use of the test-year is justifiable. The discontinuities between months should not affect the statistical analysis significantly, as the potential rapid changes in temperature and humidity affect the surface conditions only during the first couple of hours in each month.

The use of models in this study is justifiable as well. Every model used here has been verified and the verification done along this study proves that the results represent wintertime meteorological condition fairly well, although the modelled night time temperature is slightly colder than it should be. The comparison between RoadSurf, SURFEX and 2014–2015 road weather observations further proves that RoadSurf is capable of predicting the road conditions accurately.

The delta-change method doesn't take into account the fact that the frequency distribution of temperature tends to peek at the freezing point. Adding the delta-change to every point shifts this peak couple degrees above freezing. As the difficult traffic and pedestrian conditions are common near freezing temperature, the number of difficult condition could be actually higher than the results predict.

The methods for creating longwave radiation data for the future climate and calculating snow/precipitation proportion were developed in this study. These methods function well enough for this study, but they could be further improved. Dividing the longwave-humidity data points to two linear data sets does not describe the meteorological conditions perfectly, but it is close enough as the amount of data points between the lines is quite small. In a future study, these points between the lines could still be preserved, though, if instead of the whole linear fits only the slopes would be used. For every data point it could be determined whether the point is above or below the average line as shown in figure 10, but then the projection to the future climate would be determined based on the original data point location and the slope of above or below fit. This way every point would be projected along its own fit and the variation seen in figure 10a would be preserved.

The use of linear fit to calculate the snow proportion of total precipitation is overly simplified and by using this method we lose the divergence in snow proportion near the freezing point seen in figure 9. These different snow and water ratios can affect the road weather significantly, but in this study the effect is minimal. This is due to the fact that this ratio is used only when calculating the precipitation input for SURFEX/TEB. For RoadSurf the precipitation input is given as total precipitation. Therefore the ratio affects directly only the SURFEX/TEB modelling, and RoadSurf output is affected only indirectly through the ground level temperature calculated in SURFEX/TEB. For the same reason, using more complex fit instead of linear fit would not have added much more value to the results.

According to the modelled results, both difficult traffic and pedestrian weather conditions decrease significantly when moving to the 2040–2069 climate. It should be noted, though, that RoadSurf does not take the road maintenance into account if the 100 cm snow depth threshold is not exceeded. Therefore, the amount of difficult cases is overestimated and would likely decrease with realistic road maintenance. On the other hand, the different indexes don't take into account the darkness, which in some cases can cause as difficult conditions as the ones related to snow. Especially in wintertime, evenings can be very dark if there is no snow cover. These dark conditions would very likely increase due to the decreased snow portion of the total precipitation.

These results can be used to assess the need of road maintenance in the mid of 21st century in the Helsinki capital region, but the limitations of the method should be taken into account. It is not clear that the decreases in the difficult road and pedestrian conditions would be linear. The number of these conditions could even increase at first when the temperature rises, and for this reason these results can be used to assess the average conditions only in 2040–2069. The location is significant as well, as these results would very likely be different in other cities.

To further assess the development of the difficult road and pedestrian conditions in changing climate, this study should be repeated with a different time horizon, preferably with 2020-2049 as the future climate. Other RCP-scenarios should also be considered to assess the impact of climate change -preventing actions on road conditions. Simulations for other Finnish cities, for example Jyväskylä and Sodankylä, could be used to increase the coverage of these results to central and northern parts of Finland.

Project URCLIM is part of ERA4CS, an ERA-NET initiated by JPI Climate, and funded by FORMAS (SE), DLR (DE), BMWFW (AT), IFD (DK), MINECO (ES), ANR (FR)* with co-funding by the European Union (Grant 690462). Partially funded by the Academy of Finland through the PLUMES project (Pathways Linking Uncertainties in Model Projections of Climate and its Effects; decision number 278067).

iSCAPE has received funding from the European Community's H2020 Programme under Grant Agreement No. 689954.

References

[1] I. Juga et al. "Analysis of weather factors responsible for the traffic 'Black Day' in Helsinki, Finland, on 17 March 2005". In: *Meteorological Applications* 19 (2012), pp. 1–9.

[2] M. Hippi and S. Hartonen. "Statistical data of slipping injuries happened in the winter time". In: *SIRWEC 2012 International Road Weather Conference in Helsinki*. 2012.

[3] R. Hautala and P. Leviäkangas. *Ilmatieteen laitoksen palveluiden vaikuttavuus. Hyötyjen arviointi ja arvottaminen eri hyödyntäjä-toimialoilla*. Vol. 665. Espoo: VTT Publications, 2007.

[4] E. Räty and T. Kari. *Vakuutusyhtiöiden liikennevahinkotilasto 2017*. Helsinki: The Finnish Crash Data Institute (Onnettomuustietoinstituutti), Nov. 2018.

[5] J. Sipilä and O. Mäkelä. *Talvihoidon suoritteet ja kustannukset eri tietyypeillä*. Finnish National Road Administration (Tiehallinto), 2006.

[6] J. Rissanen and P. Häkkinen. *Talvikunnossapito 2016,Talven vaikeusaste ja saavutettu laatutaso*. Tampere: City of Tampere, June 2016.

[7] S. Saarelainen and L. Makkonen. *Ilmastonmuutokseen sopeutuminen tienpidossa*. Tiehallinnon selvityksiä. Helsinki: Finnish Road Administration (Tiehallinto), Apr. 2007.

[8] V. Männisto. *Talvikunnossapito 2016,Talven vaikeusaste ja saavutettu laatutaso*. Tiehallinnon selvityksiä. Helsinki: Finnish Road Administration (Tiehallinto), Aug. 2006.

[9] Project iSCAPE. *About iSCAPE*. `https://www.iscapeproject.eu/about/`. Accessed on 20.5.2019.

[10] Project iSCAPE. *iSCAPE Living Labs*. `https://www.iscapeproject.eu/iscape-living-labs/`. Accessed on 20.5.2019.

[11] JPI Climate. *URCLIM*. `http://www.jpi-climate.eu/nl/25223460-URCLIM.html`. Accessed on 20.5.2019.

[12] D. L. Hartmann. *Global Physical Climatology*. Vol. 56. International Geophysics. London: Academic Press Limited, 1994.

[13] T. R. Oke et al. *Urban Climates*. Cambridge University Press, 2017.

[14] P. Bauer, A. Thorpe, and G. Brunet. "The quiet revolution of numerical weather prediction". In: *Nature* 525 (Sept. 2015), pp. 47–55.

[15] E. Kalnay. *Atmospheric modeling, Data Assimilation and Predictability*. New York: Cambridge University Press, 2002.

[16] A. C. Lorenc. "Analysis methods for numerical weather prediction". In: *Quarterly Journal of the Royal Meteorological Society* 112 (1986), pp. 1177–1194.

[17] R. Moss et al. *Towards New Scenarios for Analysis of Emissions, Climate Change, Impacts, and Response Strategies*. IPCC Expert Meeting Report. Geneva: Intergovernmental Panel on Climate Change, 2008.

[18] D.P. van Vuuren et al. "The representative concentration pathways: an overview". In: *Climatic Change* 109 (2011), pp. 5–31.

[19] L. Clarke et al. "International climate policy architectures: Overview of the EMF 22 International Scenarios". In: *Energy Economics* 31 (2009), pp. 64–81.

[20] K. Ruosteenoja, K. Jylhä, and M. Kämäräinen. "Climate projections for Finland under the RCP forcing scenarios". In: *Geophysica* 51 (2016), pp. 17–50.

[21] K. Jylhä et al. "Rakennusten energialaskennan testivuosi TRY2012 ja arviot ilmastonmuutoksen vaikutuksista". In: *Ilmatieteen laitos, Raportteja* 6 (2011).

[22] M. Kangas, M. Heikinheimo, and M. Hippi. "RoadSurf - a modelling system for predicting road weather and road surface conditions". In: *Meteorological Applications* 22(3) (2015), pp. 544–553.

[23] R. Ruuhela, J. Ruotsalainen, and M. Kangas. "Kelimallin kehittäminen talvijalankulun turvallisuuden parantamiseksi". In: *Ilmatieteen laitos, Raportteja* 1 (2005).

[24] M. Hippi. "Monitoring slipperiness on walkways". In: *SIRWEC 2012 International Road Weather Conference in Helsinki*. 2012.

[25] V. Masson et al. "The SURFEXv7.2 land and ocean surface platform for coupled or offline simulation of earth surface variables and fluxes". In: *Geoscientific Model Development* 6 (2013), pp. 929–960.

[26] V. Masson. "A Physically-based Scheme for the Urban Energy Budget in Atmospheric Models". In: *Boundary-Layer Meteorology* 94 (2000), pp. 357–397.

[27] S. Faroux et al. "ECOCLIMAP-II/Europe: a twofold database of ecosystems and surface parameters at 1 km resolution based on satellite information for use in land surface, meteorological and climate models". In: *Geoscientific Model Development* 6 (Apr. 2013).

[28] L. Bengtsson et al. "The HARMONIE-AROME Model Configuration in the ALADIN-HIRLAM NWP System". In: *Monthly Weather Review* 145 (2017), pp. 1919–1935.

[29] Finnish Meteorological Institute. *Sääennustedata*. `https://ilmatieteenlaitos.fi/avoin-data-saaennustedata-hirlam`. Accessed on 20.5.2019, in Finnish.

[30] J. Vinha et al. *Ilmastonmuutoksen ja lämmöneristyksen lisäyksen vaikutukset vaipparakenteiden kosteusteknisessä toiminnassa ja rakennusten energiankulutuksessa*. Tampere: Tampere University of Technology, 2013.

[31] NASA. *Clouds and Radiation*. `https://earthobservatory.nasa.gov/features/Clouds`. Accessed on 20.5.2019.

[32] K. Jylhä et al. "Energy demand for the heating and cooling of residential houses in Finland in a changing climate". In: *Energy and Buildings* 99 (2015), pp. 544–553.

[33] Finnish Meteorological Institute. *Rakennusfysiikan ilmastolliset testivuodet*. `https://ilmatieteenlaitos.fi/rakennusfysiikan-ilmastolliset-testivuodet`. Accessed on 20.5.2019. June 2014.

[34] R. Daley. *Atmospheric data analysis*. Press Syndicate of the University of Cambridge, 1991.